QUENCHING OF OXALYL FLUORIDE (^3A_u) MOLECULES

R. R. KARL, Jr., F. B. WAMPLER, R. C. OLDENBORG and W. W. RICE

University of California, Los Alamos Scientific Laboratory, Los Alamos, N.M. 87545
(U.S.A.)

Summary

Rate constants for quenching of oxalyl fluoride (^3A_u) molecules by selected classes of quenchers have been investigated using the technique of laser-induced time-resolved phosphorescence. Various inorganic, alkane, halogenated alkane, alkene, halogenated alkene, diene and alkyne quenchers were studied. NO was found to have a much larger quenching rate constant than O_2 (6.8×10^{10} and 1.4×10^8 l mol^{-1} s^{-1} respectively). The alkane data are consistent with a hydrogen atom abstraction mechanism. Both alkene and halogenated alkene rate constants were found to increase as the triplet energy of the particular quencher decreased. Similar correlations of rate constants and triplet energy levels were found for the diene and alkyne compounds studied. The phosphorescence emission spectrum was recorded and the ^3A_u state of oxalyl fluoride was found to lie at 85.6 kcal mol^{-1}. A single progression in the ground state ν_1 (C=O symmetric stretch) is the dominant feature of the spectrum.

1. Introduction

Several papers have appeared recently which focus on the dynamics of electronically excited gas phase dicarbonyls [1 - 11]. We have had an interest in examining the dynamics of this class of compounds and have investigated the quenching reactions of 2,4-pentadione [6] which can undergo tautomerism in the gas phase and also have studied biacetyl ^3A_u molecules [5] which have a very low triplet energy of 57.2 kcal mol^{-1} [12]. Recently we reported our preliminary results on oxalyl fluoride ^3A_u molecules [13] and have now extended in detail our study of this triplet dicarbonyl which has the unusual property of possessing a triplet level whose energy lies at 85.6 kcal mol^{-1}.

The present work details our results for quenching of oxalyl fluoride ^3A_u molecules by various inorganic quenchers, alkanes, halogenated alkanes, alkenes, dienes and acetylene. Mechanistic routes are developed which are consistent with our quenching results.

2. Experimental

A schematic diagram of the experimental apparatus is shown in Fig. 1. A CMX-4 flashlamp-pumped dye laser operating with rhodamine 6-G is frequency doubled to yield 298 nm radiation having a bandwidth of 5.4 cm^{-1}. The pulsed output energy is about 0.1 mJ with a duration of about 1 μs. The fundamental frequency is filtered out before the laser beam enters the Pyrex fluorescence cell of radius 4 cm fitted with Suprasil windows. A RCA C31034A photomultiplier tube is positioned perpendicular to the laser beam and appropriate beam apertures were positioned in the cell to discriminate against scattered light. A Corning 5-59 filter is placed in the $F/1.5$ collection optics and phosphorescence in the 304 - 510 nm spectral region is monitored. A Pacific Photometric Model 2A44 preamplifier in the tube housing feeds the signal into a Tektronix 7844 oscilloscope and the resulting phosphorescence intensity traces are photographed. The decays are found to be single exponentials. The intensities are strong enough that lifetimes can be measured from a single trace. Twenty scope traces are recorded and averaged photographically. The Pyrex fluorescence cell, stainless steel sample mixing cylinders and delivery lines are evacuated via a liquid-nitrogen-trapped diffusion pump to 10^{-6} Torr and the outgassing rate is shown to be less than 10^{-5} Torr min^{-1}. The samples are condensed with liquid nitrogen and pumped on to remove volatile impurities; those containing inhibitors or known impurities are distilled trap-to-trap for purification just prior to use. The data are recorded with 5.00 Torr of oxalyl fluoride at 24 - 28 °C with various pressures of added quenchers to change the $1/\tau$ values observed from 3 × 10^3 s^{-1} to 2 × 10^4 s^{-1}. The pressures required to obtain this range of $1/\tau$ values vary significantly among the different quenchers. The
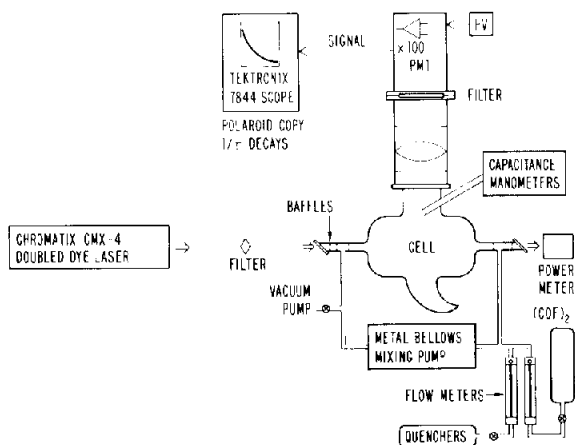

Fig. 1. Experimental apparatus showing the baffled Pyrex phosphorescence cell with Suprasil windows and the PMT detector system with $F/1.5$ light gathering optics and filter.

more efficient quenchers that give rate constants over 10^8 l mol^{-1} s^{-1} are diluted with argon to facilitate more precise measurement of all the small quantities of added gas. Dilution by factors of 10^1 - 10^4 is performed in the sample cylinders and allowed to mix by diffusion for at least three hours prior to use. The rate correction for argon dilutant is insignificant in all cases and therefore disregarded. Pressures are measured using MKS Baratron capacitance manometers of optimum full scale ranges. After each addition of a quencher the contents of the fluorescence cell are mixed with a stainless steel Metal Bellows pump circulation loop to ensure uniformity of the two gases. A series of experiments were performed with a constant flowing oxalyl fluoride pressure while attenuating the laser energy with neutral density filters and each experiment gave the same $1/\tau$ values. This verified that the laser excited a sufficiently minor number of the molecules and that any triplet–triplet (T–T) interaction can be disregarded.

The phosphorescence spectrum is recorded using 5 Torr of pure oxalyl fluoride and the laser is operated at 15 pulses s^{-1}. The gas is flowed and replenished so that a fresh sample is always being irradiated. The fluorescence signal is very effectively removed from the phosphorescence recording by integrating 100 μs of gate width beginning 25 μs after the laser pulse using a Princeton Applied Research Model 162 boxcar integrator. A $\frac{1}{8}$ m Oriel 7240 grating monochrometer is inserted after the light collection lens with its slit length parallel to the laser beam passing through the phosphorescence cell. The spectrum shown in Fig. 2 was recorded at 1.0 nm bandpass.

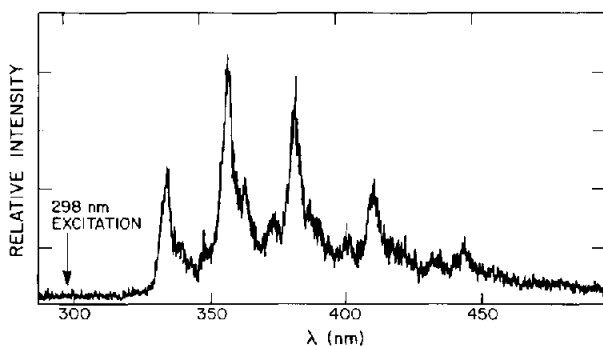All chemicals were of high purity and were obtained from commercial vendors.

Fig. 2. Phosphorescence emission spectrum of oxalyl fluoride recorded 25 - 125 μs after excitation at 298 nm.

3. Results and discussion

Figure 2 shows the phosphorescence emission spectrum of oxalyl fluoride. The spectrum is dominated by what is apparently a single vibrational progression. The spacings between the peaks in this progression vary from 1810 to 1840 cm^{-1}. Other smaller features are discernable with spacings of 1420, 1110 and 860 cm^{-1}.

From the oxalyl fluoride fluorescence self-quenching rate constant measured by Baronavski and McDonald [9], we estimate a fluorescence lifetime of about 10 ns at 5 Torr. This short fluorescence lifetime combined with the 25 μs delay before sampling the emission assure that the phosphorescence spectrum is essentially free of all fluorescence. In addition, during that long delay time an excited triplet molecule experiences enough collisions with unirradiated molecules effectively to relax any excess vibrational excitation and leave all triplet molecules in their ground vibrational state.

The largest change in geometry between the ground ^1A_g and excited ^3A_u states is an extension of the C=O bond length in the triplet state. Progressions in the symmetric C=O stretching mode would be expected to dominate the spectrum [14]. The energy of this mode in the ground electronic state has been measured as 1872 cm^{-1} in Raman spectra of liquid phase oxalyl fluoride [15]. It is therefore reasonable to assign the dominant progression in our spectrum as being a progression in the ground state symmetric C=O stretch originating in the vibrational ground state of the triplet. The shortest wavelength peak of the progression lies at 334 nm and should represent the band origin. This is in excellent agreement with the 29 942 cm^{-1} band origin for the ^3A_u - ^1A_g system measured by Balfour and King [14] in their high resolution ultraviolet absorption studies. This places the ^3A_u energy level at 85.6 kcal mol^{-1}.

Let us consider the decay processes of oxalyl fluoride (^3A_u) molecules immediately after their production from the excited singlet manifolds:

$$^3(COF)_2 \rightarrow (COF)_2 + h\nu_p \tag{1}$$

$$^3(COF)_2 \rightarrow (COF)_2 \tag{2}$$

$$^3(COF)_2 + (COF)_2 \rightarrow \text{Removal} \tag{3}$$

$$^3(COF)_2 + M \rightarrow \text{Removal} \tag{4}$$

where $h\nu_p$ indicates phosphorescence emission and M is a foreign quencher. The following equation is valid to describe the kinetic scheme:

$$\frac{-d[^3(COF)_2]}{dt[^3(COF)_2]} = \frac{1}{\tau} = k_1 + k_2 + k_3[(COF)_2] + k_4[M] \tag{5}$$

Equation (5) is the familiar Stern–Volmer equation and a plot of $1/\tau$ versus [M] for a fixed $(COF)_2$ concentration should be linear in [M]. This relationship was followed for all of the quenchers in the present study and represen-

tative Stern–Volmer plots are shown in Figs. 3 - 5. Table 1 summarizes the
rate constants k_4 determined for each of the quenchers studied.

Let us first consider the quenching rate constants obtained for the in-
organics. The low rate constants obtained for H_2 and Ar (1.1×10^4 and
2.7×10^4 l mol^{-1} s^{-1} respectively) are indicative of the absence of any effi-
cient chemical or physical quenching channel. The quenching is most likely
due to collisional deactivation which proceeds more rapidly with the larger
Ar atom than with the smaller H_2. The self-quenching route proceeds much
more efficiently than with H_2 or Ar. However, the self-quenching rate
constant of 1.1×10^7 l mol^{-1} s^{-1} is significantly below the self-quenching
rate constant for glyoxal, 2.16×10^8 l mol^{-1} s^{-1} [4]. This is most likely due
to the chemical inertness of C–F bonds on oxalyl fluoride and diminishes
the attractiveness of chemical quenching channels which are thought to
occur with glyoxal self-quenching [4]. The quenching of the oxalyl fluoride
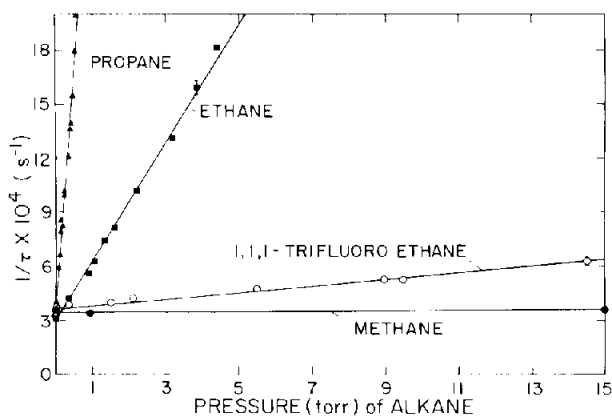triplet by O_2 can occur via the following spin-allowed reaction:

Fig. 3. Stern–Volmer plots for representative alkanes: (COF)$_2$ pressure, 5.00 Torr;
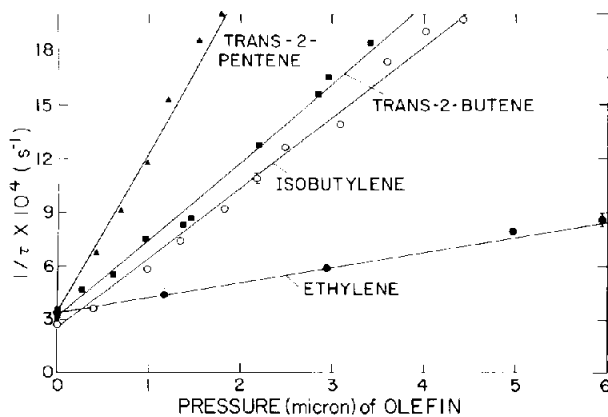excitation wavelength, 298 nm.

Fig. 4. Stern–Volmer plots for representative halogenated alkenes. (COF)$_2$ pressure,
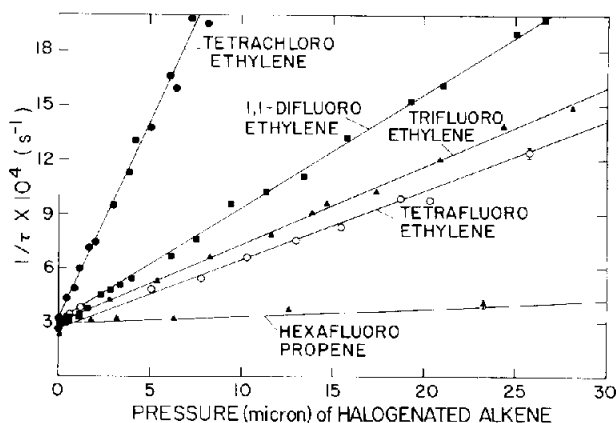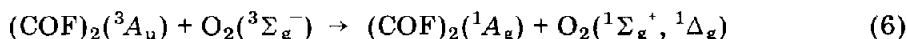5.00 Torr; excitation wavelength, 298 nm.

Fig. 5. Stern–Volmer plots for representative halogenated alkenes: $(COF)_2$ pressure, 5.00 Torr; excitation wavelength, 298 nm.

$$(COF)_2(^3A_u) + O_2(^3\Sigma_g^-) \rightarrow (COF)_2(^1A_g) + O_2(^1\Sigma_g^+, {}^1\Delta_g) \tag{6}$$

The rate constant for O_2 quenching (1.4×10^8 l mol^{-1} s^{-1}) is in reasonable agreement with the estimate that can be derived from the empirical fit by Calvert et al. [16] for O_2 quenching rate constants versus the triplet energy level of the donors. The quenching by NO probably proceeds via a spin-allowed doublet transition state as suggested by Gijzeman et al. [17]. They have noted a very large increase for NO quenching of triplets when the triplet level lies above 42.9 kcal mol^{-1} and have developed a theoretical interpretation in terms of their spin-allowed model to explain this trend successfully. Our very large quenching rate constant for NO (6.8×10^{10} l mol^{-1} s^{-1}) suggests that this same favorable mechanism is a reasonable channel for NO quenching.

The quenching reactions of the alkanes and halogenated alkanes may be consistent with some form of hydrogen abstraction reaction channel. CH_4, C_2H_6 and C_3H_8 have rate constants of 3.1×10^5 l mol^{-1} s^{-1}, 6.4×10^7 l mol^{-1} s^{-1} and 5.1×10^8 l mol^{-1} s^{-1} respectively, which is similar to the trend we would anticipate for hydrogen abstraction by the $(COF)_2$ triplet. For example, when SO_2 $(^3B_1)$ molecules abstract hydrogen atoms from CH_4, C_2H_6 and C_3H_8, the chemical quenching rate constants are 3.35×10^6 l mol^{-1} s^{-1}, 3.09×10^7 l mol^{-1} s^{-1} and 2.33×10^8 l mol^{-1} s^{-1}, respectively [18]. This trend is in accordance with the decrease in the C–H bond energy in going from CH_4 to C_2H_6 to C_3H_8. The present oxalyl fluoride quenching rate constants by the previously mentioned alkanes contain some undefined physical quenching component but the trend noted is quite suggestive that a chemical quenching channel dominates. One piece of information to support this concept is noted by comparing the quenching rate constants for CH_4 and CF_4 (3.1×10^5 l mol^{-1} s^{-1} and 1.7×10^5 l mol^{-1} s^{-1} respectively). If collisional deactivation were the dominant quenching channel for CH_4 as it

TABLE 1

Rate constants determined at room temperature for removal of oxalyl fluoride ^3A_u molecules

Quencher, M	k_4 (l mol^{-1} s^{-1})
(a) Inorganics	
Hydrogen	1.1×10^4
Argon	2.7×10^4
Carbonyl fluoride	1.1×10^7
Oxygen	1.4×10^8
Nitric oxide	6.8×10^{10}
(b) Alkanes and halogenated alkanes	
Methane	3.1×10^5
Ethane	6.4×10^7
Propane	5.1×10^8
Tetrafluoromethane	1.7×10^5
1,1,2,2-Tetrafluoroethane	1.8×10^6
1,1,2-Trifluoroethane	2.0×10^6
1,1,1-Trifluoroethane	3.3×10^6
(c) Alkenes	
Ethylene	1.5×10^{10}
Isobutylene	7.6×10^{10}
trans-2-Butene	8.3×10^{10}
cis-2-Butene	9.7×10^{10}
trans-2-Pentene	1.7×10^{11}
cis-2-Pentene	2.0×10^{11}
(d) Halogenated alkenes	
Hexafluoropropene	7.6×10^8
Tetrafluoroethylene	7.0×10^9
Trifluoroethylene	8.2×10^9
cis-1,2-Difluoroethylene	9.4×10^9
trans-1,2-Difluoroethylene	9.5×10^9
Vinyl fluoride	1.0×10^{10}
1,1-Difluoroethylene	1.2×10^{10}
Chlorotrifluoroethylene	1.4×10^{10}
1,1-Dichloro-2,2-difluoroethylene	1.6×10^{10}
Tetrachloroethylene	4.0×10^{10}
(e) Dienes	
Perfluoro-1,3-butadiene	1.1×10^{10}
1,3-Butadiene	1.7×10^{11}
(f) Alkynes	
Acetylene	3.6×10^9

undoubtedly is for CF_4, then the smaller CH_4 molecule would be expected to have a smaller rate constant than CF_4. Also complementary to the suggestion of a hydrogen abstraction mechanism is our observed rate constant values for quenching by CF_2H-CF_2H (1.8×10^6 l mol^{-1} s^{-1}), CF_2H-CFH_2 (2.0×10^6 l mol^{-1} s^{-1}) and CF_3-CH_3 (3.3×10^6 l mol^{-1} s^{-1}). The fluorinated ethanes containing three hydrogens quench more efficiently than

those containing two hydrogens. CF_2H-CFH_2 contains three hydrogens but its quenching constant is less than CF_3-CH_3 which also contains three hydrogens. This is most likely due to fluorine atom repulsions and also steric hindrance from the fluorine atom to diminish the accessibility of the hydrogen atom on CF_2H-CFH_2 relative to CF_3-CH_3 where one entire end of the substituted ethane contains only hydrogen atoms.

Let us now focus our attention on the unsaturated hydrocarbon quenchers. Triplet–triplet energy transfer is known to occur with unsaturated hydrocarbons and triplet donors. Rebbert and Ausloos [19] have successfully correlated increasing quenching rate constants for triplet acetone with the increasing exothermicity of the triplet–triplet transfer. It appears that the alkenes in the present study follow this same trend. The vibrationally relaxed triplet energy E_T for C_2H_4 has been estimated to lie 82 kcal mol^{-1} above its vibrationally relaxed ground state [20, 21]. E_T for isobutylene probably lies near that of *cis*- and *trans*-2-butene which lie at 76 and 70 ± 2 kcal mol^{-1} [22] respectively. E_T for *trans*- and *cis*-2-pentene would be anticipated to lie slightly below E_T for *trans*- and *cis*-2-butene since additional alkyl substitution of the mono-olefins is thought to result in lower triplet energy levels [19]. Note that the decreasing E_Ts in proceeding from ethylene to the 2-pentenes result in increasing rate constants for quenching of the $(COF)_2$ (^3A_u) state which has E_T = 85.6 kcal mol^{-1}.

The halogenated alkene quenching rate constants also can be explained via a T–T energy transfer mechanism. While not all the E_Ts are known, enough information is available to predict trends in E_T. From Moore's work [21] on ion impact energy loss spectroscopy it can be deduced that E_T decreases relative to C_2H_4 when a substituted ethylene contains chlorine atoms and increases when it contains fluorine atoms. For example, from Moore's data we can use the threshold for scattering due to energy loss to estimate E_T = 82 kcal mol^{-1} for C_2H_4, E_T = 76 kcal mol^{-1} for C_2H_3Cl and E_T = 89 kcal mol^{-1} for C_2H_3F. It also seems that increasing fluorination increases E_T and that increasing chlorination decreases E_T for substituted ethylenes. It can be noted from Table 1 (d) that C_2Cl_4 has the highest quenching rate constant (4.0×10^{10} l mol^{-1} s^{-1}) and that as we progress down to $CF_3-CF=CF_2$ (the most fluorinated ethylene derivative studied) the rate constant decreases to 7.6×10^8 l mol^{-1} s^{-1}. On replacing the CF_3 group on hexafluoropropene with a fluorine atom to yield C_2F_4, the quenching rate constant increases by almost an order of magnitude. As we progress in Table 1 (d) from C_2F_4 towards C_2Cl_4, quenching rate constants agree for the most part with predicted trends in E_T; however, completely definitive correlations cannot be deduced because of a lack of information on E_T values.

Inspection of our rate constants for dienes and alkynes further supports the T–T energy transfer mechanism for oxalyl fluoride (^3A_u) molecules and unsaturated hydrocarbons if we consider the value of their triplet energy levels.

An average literature value of E_T = 59.7 kcal mol^{-1} for 1,3-butadiene can be estimated from the work of Evans [20] (E_T = 59.6 kcal mol^{-1}) and

from Kellogg and Simpson [23] (E_T = 59.8 kcal mol^{-1}). Based upon the previously mentioned comments regarding fluorine substitution, E_T for perfluoro-1,3-butadiene would be expected to lie significantly above 59.8 kcal mol^{-1}. The large value for the 1,3-butadiene quenching rate constant is in agreement with what would be anticipated since its triplet lies so low relative to oxalyl fluoride. Also the decrease in the quenching rate constant for perfluoro-1,3-butadiene relative to 1,3-butadiene is in accordance with the predicted higher E_T. The E_T for acetylene has been estimated to be 92 kcal mol^{-1} [19]. Note that C_2H_2 has a rate constant of 3.6×10^9 l mol^{-1} s^{-1} and this fits nicely with the fact that its T–T transfer is endothermic and is thus expected to be significantly lower than those quenchers which may undergo exothermic T–T transfer.

In conclusion, the quenching rate constant of the ^3A_u state of oxalyl fluoride varies dramatically with the chemical identity and/or triplet level of the quencher. Since the triplet level of oxalyl fluoride (E_T = 85.6 kcal mol^{-1}) is very high, it has the ability to undergo efficient T–T energy transfer with a large number of unsaturated hydrocarbons. Furthermore, the oxalyl fluoride triplet can undergo chemical quenching with alkanes to abstract hydrogen atoms. The familiar triplet quenchers O_2 and NO have significantly different rate constants for removal of the ^3A_u state of oxalyl fluoride (1.4×10^8 and 6.8×10^{10} l mol^{-1} s^{-1} respectively). Inert inorganic gases which have no available energy transfer mechanism, as do O_2 and NO, are limited to collisional deactivation processes and may have rate constants as low as the 1.1×10^4 l mol^{-1} s^{-1} noted for H_2 quenching.

Acknowledgments

References

1 H. W. Sidebottom, C. C. Badcock, J. G. Calvert, B. R. Rabe and E. K. Damon, *J. Am. Chem. Soc., 94* (1972) 13.
2 C. S. Parmenter and H. M. Poland, *J. Chem. Phys., 51* (1969) 1551.
3 A. F. Moss and J. T. Yardley, *J. Chem. Phys., 61* (1974) 2883.
4 J. T. Yardley, *J. Chem. Phys., 56* (1972) 6192.
5 F. B. Wampler and R. C. Oldenborg, *Int. J. Chem. Kinet., 12* (1978) 1225.
6 F. B. Wampler and R. C. Oldenborg, *J. Photochem., 8* (1978) 273.
7 M. E. Garabedian and D. A. Dows, *J. Am. Chem. Soc., 90* (1968) 2468.
8 R. W. Carr, Jr., and M. P. Ramirez, *J. Photochem., 6* (1976) 431.
9 A. P. Baronavski and J. R. McDonald, *J. Chem. Phys., 67* (1977) 4286.
10 C. S. Parmenter and B. L. Ring, *J. Chem. Phys., 46* (1967) 1998.
11 R. A. Coveleskie and J. T. Yardley, *J. Am. Chem. Soc., 97* (1975) 1667.
12 R. vanderWerf and J. Kommandeur, *Chem. Phys., 9* (1976) 125.

13 R. R. Karl, Jr., F. B. Wampler, R. C. Oldenborg and W. W. Rice, *J. Photochem.*, *9* (1978) 407.
14 W. J. Balfour and G. W. King, *J. Mol. Spectrosc.*, *25* (1968) 130.
15 J. L. Hencher and G. W. King, *J. Mol. Spectrosc.*, *16* (1965) 168.
16 J. G. Calvert, F. Su, J. W. Bottenheim and O. P. Strauz, *Atmos. Environ.*, *12* (1978) 197.
17 O. L. J. Gijzeman, F. Kaufman and G. Porter, *J. Chem. Soc. Faraday Trans. II*, *69* (1974) 727.
18 F. B. Wampler, R. C. Oldenborg, W. W. Rice and R. R. Karl, Jr., *J. Chem. Phys.*, *69* (1978) 2569.
19 R. E. Rebbert and P. Ausloos, *J. Am. Chem. Soc.*, *87* (1965) 5569.
20 D. F. Evans, *J. Chem. Soc.*, (1960) 1735.
21 J. H. Moore, Jr., *J. Phys. Chem.*, *76* (1972) 1130.
22 R. D. Penzhorn and H. Güsten, *Z. Naturforsch.*, *27* (1972) 1401.
23 R. E. Kellogg and W. T. Simpson, *J. Am. Chem. Soc.*, *87* (1965) 4230.